

ZACHARY M. BYKO*, PAUL MARKOWSKI, AND YVETTE P. RICHARDSON

Department of Meteorology, Pennsylvania State University, University Park, PA

JOSHUA WURMAN

Center for Severe Weather Research, Boulder, CO

1. Introduction

Hook echoes and their associated rear-flank dowrafts are well-known to be closely associated with the development of near-ground rotation in supercells, a prerequisite for tornado-genesis. Fujita (1958), in a study of the Champaign, IL tornado of 9 April 1953, illustrated the formation of the appendage, commonly referred to as the hook echo, observed in radar observations of supercells. At the time, Fujita hypothesized that the hook echo formed as precipitation was advected around a supercell’s rotating updraft. Browning (1964, 1965) also did pioneering work on supercells and hook echoes. Figure 1 (from Browning 1965) schematically depicts the appearance of a supercell and development of the hook echo on radar that occurred on 26 May 1963 near Oklahoma City. Browning (1965) described the embryonic hook as a “finger of echo” at the rear of the supercell. Due to the rotating updraft, the finger begins to turn toward the storm’s right flank and is then called a pendant echo (Browning 1965). As the leading edge of the pendant echo continues to curl cyclonically, a classic hook echo is formed. The idea that a hook echo forms as hydrometeors from a supercell’s main echo region are advected toward the storm’s rear by the rotating updraft has generally been accepted for the past 40 years.

Garrett and Rockney (1962) noted that small echo dots, termed “annular sections of a storm vortex cylinder” (asc’s), were occasionally located at the tip of a hook echo and believed these dots to be a radar representation of debris resulting from a tornado. However, it has been shown in a study of storms from the Super Outbreak of 1974 that a majority of echo dots were not accompanied by a tornado, thus it is unlikely they are a radar signature of debris (Forbes 1981). Forbes (1981) also stated that some of the echo dots morphed into the hook echo itself.

Rasmussen et al. (2006), hereafter RSGD06, show examples of hook echoes that form when descending reflectivity cores (DRCs) reach the low levels. It has been suggested that some of the asc’s previously cited in the literature may be a manifestation of the DRC (RSGD06), described as a “blob” of enhanced radar reflectivity that descends from the rear of the echo overhang in the right-rear quadrant of a supercell. RSGD06 describe the appearance of a DRC on a three-dimensional isosurface of reflectivity as a protuberance pendant from the echo

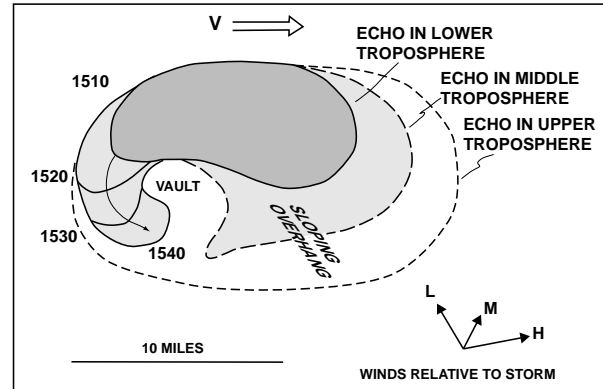


FIG. 1. Schematic diagram depicting the formation of a hook echo as observed by radar [from Browning (1965)].

overhang that descends with time (as in Fig. 2b, d, and f). On a constant elevation scan, a DRC can be identified as a localized “hot spot” of higher reflectivity initially detached from the main supercell (Fig. 2c), even though it may become attached with time, resulting in a hook echo (Fig. 2e). DRCs are accompanied by enhanced rear-to-front flow when they reach the surface, likely a result of vertical westerly momentum advection from aloft to the ground (RSGD06). One question that arises from the RSGD06 study is the degree to which observations of DRCs and hook echo formation are sensitive to the space and time resolution of the radar, as the DRCs were 100 km from the radar, on average, and sampled at 5–6 minute intervals, which is perhaps a relatively long sampling interval compared to that of today’s mobile research radars.

The purpose of this preprint is to examine mobile Doppler on Wheels (DOW) observations of DRCs. Whereas WSR-88D radars usually sample a storm over its entire depth and provide an observational context, DOW data have much finer spatial (assuming DOWs tend to be much closer to storms than a WSR-88D radar) and temporal resolution that enables a detailed picture of the formation and evolution of the hook echo and DRC in the lower levels of a supercell. In addition to the limits on the vertical extent of DOW observations, another possible weakness in using DOW data is attenuation if a storm is sampled at an unfortunate angle (i.e. through the precipitation core such that the beams pass through heavy precipitation); however, this latter limitation was not encountered in the present study.

*Corresponding author address: Zachary M. Byko, Department of Meteorology, Pennsylvania State University, 503 Walker Building, University Park, PA 16802; e-mail: zmb102@psu.edu.

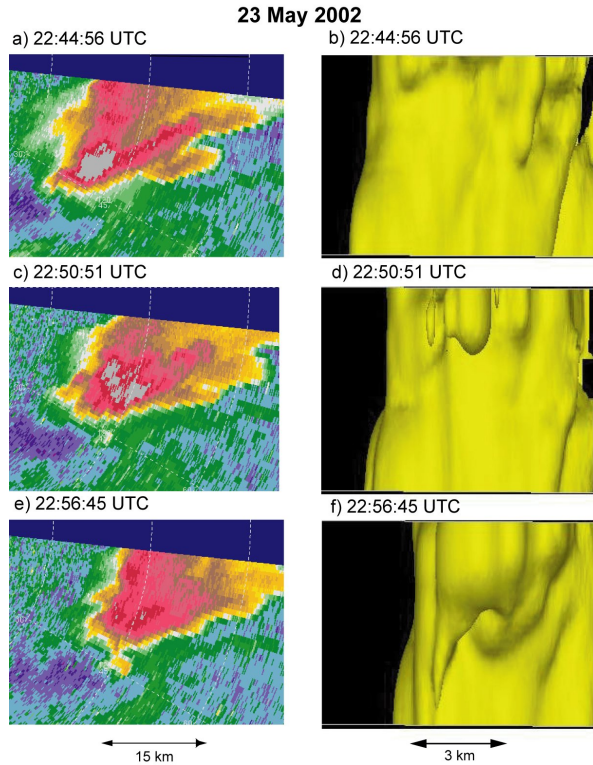


FIG. 2. Reflectivity from the 0.5° elevation scan collected by the SPOL radar at 22:44:56 UTC, 22:50:51 UTC, and 22:56:45 UTC is shown in (a), (c), and (e), respectively. The 25 dBZ reflectivity isosurfaces at the corresponding times are presented in (b), (d), and (f). The isosurfaces are viewed at an angle from the south of the storm. The arrow representing the length scale below the panels with reflectivity isosurfaces is approximately valid at the echo centroid.

2. Data and methodology

WSR-88D data collected in supercells at the time of hook echo formation were analyzed to verify the presence of a DRC. A DRC was observed by the WSR-88D in a supercell that formed on 29 May 2001 and was also observed by the DOW radars. The main diagnostic tool for determining the presence of DRCs is three-dimensional isosurface renderings of radar reflectivity. A series of these isosurfaces allows the investigator to determine if a reflectivity protuberance from the echo overhang exists and descends with time. The reflectivity isosurfaces that best elucidate the evolution of the DRC are presented here with viewing angles strategically chosen to highlight the important details. In order to create three-dimensional reflectivity isosurfaces, DOW reflectivity fields were objectively analyzed to a grid using the Barnes objective analysis scheme (Barnes 1964). The radar data generally extend upward to a height of about 2.5 km above radar level, with some variability, depending on range from the radar.

In the case of 29 May 2001, the DOW data were objectively analyzed to a Cartesian grid of dimensions $21 \times 24 \times 4$ km with a uniform grid spacing of 100 m. The smoothing parameter, κ , selected was 0.10 km^2 and the cutoff radius was 0.707 km (Pauley and Wu 1990). A reference frame correction was performed by following a reflectivity feature in time to determine

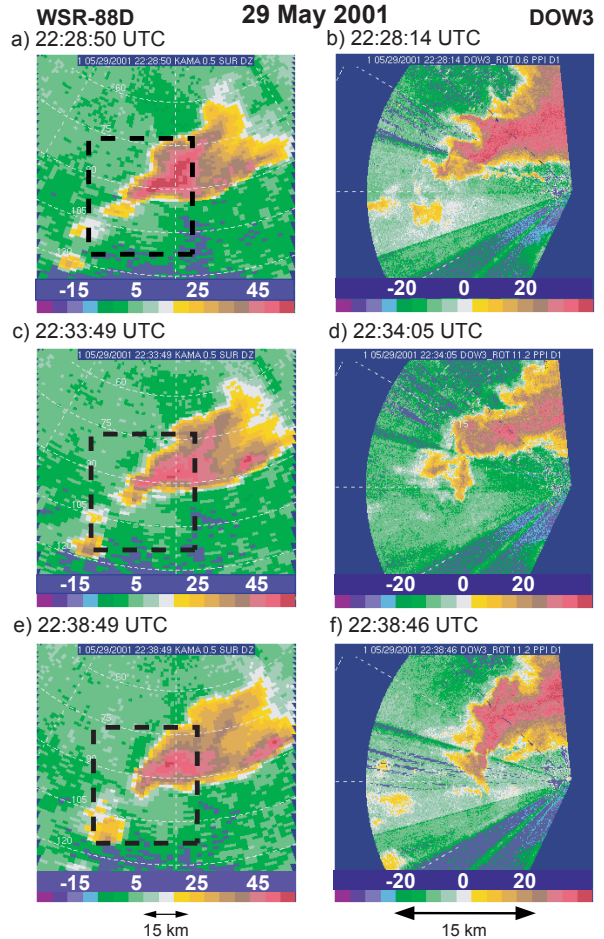


FIG. 3. 0.5° elevation scans of reflectivity from the WSR-88D at KAMA depicting hook echo formation at 22:28:50, 22:33:49, and 22:38:49 UTC in panels (a), (c), and (e), respectively. Panels (b), (d), and (f) are 1.2° elevation scans of reflectivity from DOW3 at nearly the same times. The heavy dashed box in (a), (c), and (e) indicates the DOW3 data domain.

a reference velocity, then correcting all data points in a radar volume to their position at a centralized time. The reference velocity used for the DOW data from 29 May was from 250° at 10.8 m s^{-1} .

3. Results and discussion

Figure 3 displays plan position indicator (PPI) scans of radar reflectivity from the KAMA WSR-88D and DOW3 at corresponding times on 29 May 2001. The radars depict similar DRC and hook echo evolution. Initially, a higher region of reflectivity exists near, but somewhat detached from, the main supercell echo on low elevation scans. This echo is what RSGD06 describe as the “hot spot” of higher reflectivity that appears on a constant elevation scan. Several minutes later, at about 22:34 UTC, this localized area of higher reflectivity appears to connect with the main supercell echo region. At this time, there still are several gates of higher reflectivity embedded within the early hook echo but somewhat detached from the main storm.

29 May 2001, WSR-88D

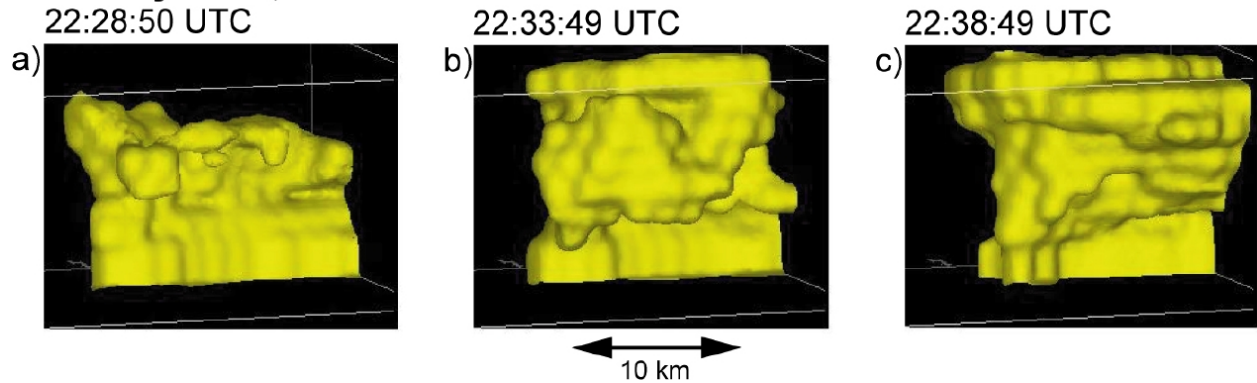


FIG. 4. A time series of the 39 dBZ reflectivity isosurface on WSR-88D data collected by the KAMA radar at the same times as in Fig. 3 (a), (c), and (e) on 29 May 2001. The view of the storm is from the southeast. The arrow representing the length scale is approximately valid at the echo centroid.

Approximately 5 minutes later, the hook echo evolution is complete, with a classic hook echo apparent on low level PPI scans.

An examination of three-dimensional reflectivity isosurfaces from the WSR-88D at the same times as the PPI data confirms the descent of a finger of higher reflectivity from the echo overhang as required of a DRC (Fig. 4). At 22:28:50 UTC, a significant area of higher reflectivity is apparent about 8 km AGL in the storm's right-rear flank (Fig. 4a). Five minutes later, this finger of reflectivity is progressing toward the ground. By 22:38:49 UTC, DRC and hook echo evolution is complete with the 39 dBZ reflectivity isosurface in Fig. 4 having an appearance very similar to the reflectivity isosurfaces presented in RSGD06.

A much more detailed account of DRC evolution in the low levels is gained by examining three-dimensional reflectivity isosurfaces from 22:29:17 through 22:32:48 UTC on 29 May 2001 from the DOW3 (Fig. 5). At 22:29:17 UTC, a relatively thin echo extension resides a few kilometers above the ground (Fig. 5a). Just over a minute later, many more of these echo extensions are present and it appears they are descending toward the ground. The appearance of the DRC as multiple cores of enhanced reflectivity on the DOW3 radar platform is likely a result of its higher resolution, which is capable of sensing reflectivity variations on a much smaller spatial scale than can the National Weather Service surveillance radar, which is at a greater range to the target. By 22:31:38 UTC, the reflectivity appendage continues its descent toward the ground and appears similar to the DRCs RSGD06 observed with WSR-88D data, having continuity in the vertical over the lowest 3 km and tapering toward the ground. By 22:32:48 UTC, the appendage has reached the ground and DRC evolution is complete (Fig. 5d).

The much finer temporal resolution afforded by DOW data allows for a more accurate determination of the DRC's evolution in the lowest few kilometers. However, it should be noted that the choice of reflectivity isosurface viewed can lead to different interpretations with regard to the evolution, and even the presence, of a DRC. Comparisons between the two radars are complicated by the fact that DOW reflectivities are uncalibrated; therefore, it is very hard to choose equivalent reflectivity isosurfaces for both. For instance, a reflectivity isosur-

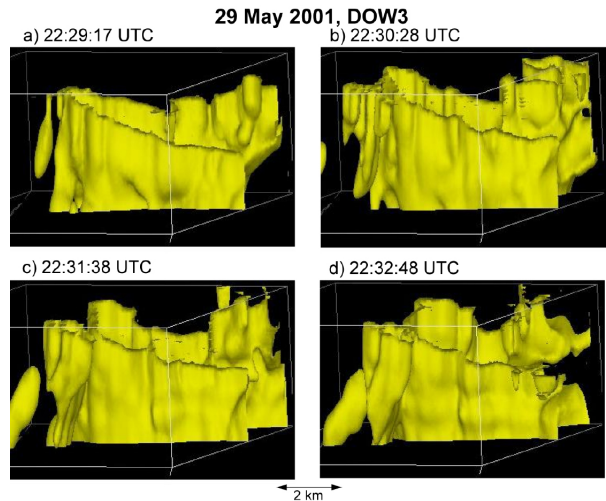


FIG. 5. A time series of the 15 dBZ reflectivity isosurface from the DOW3 on 29 May 2001 at 22:29:17 (a), 22:30:28 (b), 22:31:38 (c), and 22:32:48 UTC (d). The view of the storm is from the southeast. The arrow representing the length scale is approximately valid in the vicinity of the DRC.

face can be plotted using DOW data that shows DRC evolution complete by 22:33 UTC for the 29 May case, with the appendage reaching the ground only minutes earlier (Fig. 5). However, inspection of the 39 dBZ reflectivity isosurface from the WSR-88D suggests the DRC contacts the ground somewhere in the time range of 22:33:49 UTC and 22:38:49 UTC. Most of this time difference may be attributable to the choice of isosurface and the difficulty in choosing equivalent reflectivity isosurfaces in both the WSR-88D and DOW data. Indeed, inspection of smaller-valued reflectivity isosurfaces using WSR-88D data does indicate reflectivity present closer to the ground at 22:33:49 UTC than shown in Fig. 4. Other examples of the variability associated with isosurface choice will be examined further at the conference.

One observation of interest is the change in azimuthal shear near the ground with the descent of the DRC. An examination of azimuthal shear at 1.0 km AGL on 29 May using DOW3

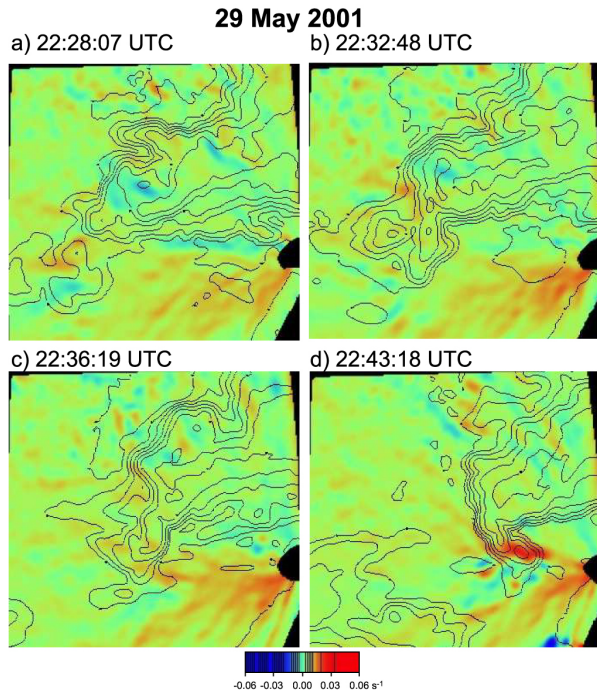


FIG. 6. A composite showing azimuthal shear (s^{-1}) (color-filled) at 1.0 km AGL and reflectivity at 1.1 km AGL (solid black contours at an interval of 8 dBZ) from the DOW3 on 29 May 2001. The times shown are 22:28:07, 22:32:48, 22:36:19, and 22:43:18 UTC in (a), (b), (c), and (d), respectively.

data shows little change in the azimuthal shear during the time of DRC descent (Figs. 6a, b). It is not until approximately 5 minutes after the DRC reaches the surface that the DOW3 data show a considerable azimuthal shear increase near the ground (Fig. 6d). This DOW-indicated increase in rotation was also observed visually at this time during the ROTATE field experiment by one of the investigators (YR). PPI scans of radar reflectivity indicate the formation of a classic hook echo happening in concert with the increase in low level azimuthal shear, likely a result of increased storm rotation deforming the shape of the radar echo (Fig. 6d). In contrast, RSGD06 found a low level rotation increase occurring simultaneously with the descent of the DRC in some cases. It is possible that the DOW3 data, with its finer temporal resolution, enabled the detection of this small time delay. The WSR-88D, given its time resolution, may be unable to sense this delay and gives the appearance of the low-level rotation increase happening concurrently with DRC arrival. This finding of a time delay between the DRC descent and the low-level azimuthal shear increase in the DOW3 data, if sampled in a significant number of other cases, may suggest a process of low-level rotation amplification that involves multiple steps (e.g. downward momentum transfer/vortex line tilting, followed by vorticity stretching).

4. Final comments and future work

DOW observations of hook echo formation, including additional observations in several cases not shown in this preprint, indicate the process can be exceedingly complex. Hook echo

formation in many instances is not only a result of hydrometeors being horizontally advected out of the main supercell echo [as concluded by Fujita (1958) and Browning (1965)] or precipitation cascading down the rear side of an updraft (as in RSGD06). Instead, some observations suggest horizontal precipitation advection and DRCs may form a continuum whereby each process contributes in varying degrees to the formation of a hook echo. This will be addressed at the conference.

Several outstanding questions should be addressed in future research. Knowledge of the physical and dynamical processes that can lead to DRC formation, or the appearance of DRC formation, must be established. A better understanding of the relative roles horizontal precipitation advection and DRCs play in hook echo formation might be of interest as well. Finally, do differences in the mechanisms by which hook echos form have significance? RSGD06 suggest that the presence of a DRC may imply a heightened tornado threat. Verification of this association could lead to an improvement in the tornado warning process.

Acknowledgments. The authors would like to thank Jeff Beck for providing his edited DOW dataset for 29 May 2001. This data set was the same one in Beck et al. that is in press at Monthly Weather Review. The contributions made by the crew of the DOWs during these missions is gratefully acknowledged. Support for this project came from NSF grants ATM-0437512 and ATM-0437505. The first author was an American Meteorological Society Graduate Fellowship recipient, sponsored by NASA's Earth Science Enterprise, for part of the time this research was conducted.

REFERENCES

- Barnes, S. L., 1964: A technique for maximizing details in numerical weather map analysis. *J. Appl. Meteor.*, **3**, 396–409.
- Browning, K. A., 1964: Airflow and precipitation trajectories within severe local storms which travel to the right of the winds. *J. Atmos. Sci.*, **21**, 634–639.
- Browning, K. A., 1965: The evolution of tornadic storms. *J. Atmos. Sci.*, **22**, 664–668.
- Forbes, G. S., 1981: On the reliability of hook echoes as tornado indicators. *Mon. Wea. Rev.*, **109**, 1457–1466.
- Fujita T. T., 1958: Mesoanalysis of the Illinois tornadoes of 9 April 1953. *J. Meteor.*, **15**, 288–296.
- Garrett, R. A., and V. D. Rockney, 1962: Tornadoes in northeastern Kansas, May 19, 1960. *Mon. Wea. Rev.*, **90**, 231–240.
- Pauley P. M., and X. Wu, 1990: The theoretical, discrete, and actual response of the Barnes objective analysis scheme for one- and two- dimensional fields. *Mon. Wea. Rev.*, **118**, 1145–1164.
- Rasmussen, E. N., J. M. Straka, M. S. Gilmore, and R. Davies-Jones, 2006: A preliminary survey of rear-flank descending reflectivity cores in supercell storms. *Wea. Forecasting.*, in press.